A First-Principles Study on the Role of Defects and Impurities in β-In_2S_3

E. Ghorbani, K. Albe

published in

NIC Symposium 2020
M. Müller, K. Binder, A. Trautmann (Editors)

Forschungszentrum Jülich GmbH,
John von Neumann Institute for Computing (NIC),
Schriften des Forschungszentrums Jülich, NIC Series, Vol. 50,
ISBN 978-3-95806-443-0, pp. 221.
http://hdl.handle.net/2128/24435

A First-Principles Study on the Role of Defects and Impurities in β-In_2S_3

Elaheh Ghorbani and Karsten Albe

Fachgebiet Materialmodellierung, Institut für Materialwissenschaft, TU Darmstadt,
Otto-Berndt-Straße 3, 64287 Darmstadt, Germany
E-mail: {ghorbani, albe}@mm.tu-darmstadt.de

CdS is a well-established buffer layer for Cu(In, Ga)(S, Se)$_2$ (CIGS)-based thin film solar cells. However, because of its toxicity, low quantum efficiency at blue-wavelength region, and the drawbacks of the chemical bath deposition technique used for its growth, looking for an alternative buffer material has been a matter of debate in recent years. In this context, β-In_2S_3 is considered as a promising substitution for CdS. β-In_2S_3 crystallises in an ordered vacancy spinel-like structure, which can accommodate impurities diffusing from the absorber and/or front contact layers. Due to the existence of structural vacancies in its crystalline matrix, the electronic and optical properties of β-In_2S_3 can be effectively tuned through (un)intentional doping with a third element. In this contribution, we will report on the origin of n-type conductivity of β-In_2S_3, the influence of Cu and Na incorporation, the thermodynamic stability and electronic properties of β-In_2S_3, and the influence of O and Cl on electronic properties of β-In_2S_3.

1 Introduction

β-In_2S_3 is an n-type semiconductor which crystallises in a defective spinel-like structure[1, 2] with four structural tetrahedral vacancies per unit cell. The interesting properties of this chalcogenide semiconductor, such as light transmission in the blue wavelength region, high open circuit voltage and fill factor qualify β-In_2S_3 for photovoltaic applications.[3] To date, the highest reported efficiencies[4] for copper indium gallium diselenide (CIGS)-based thin film solar cells have been achieved through the deposition of cadmium sulphide (CdS) as buffer layer. The major drawbacks of CdS buffer layers are: toxicity of cadmium, its conventional chemical bath deposition method, which is difficult to combine with the deposition techniques for CIGS, and its low external quantum efficiency in the short wavelength region.[5] Thus, there is an interest in replacing CdS by a transparent buffer system, which can be deposited by various techniques and has a wider band gap than CdS. This is why, there is a strong focus on β-In_2S_3 which can be deposited by various techniques[6] and has a band gap in the range of 2.0 to 2.9 eV.[1, 3, 7–9]

Due to the existence of structural vacancies, the electronic and optical properties of β-In_2S_3 can be effectively engineered and optimised through (un)intentional doping with selected atom types. Several studies have documented an intermixed In_2S_3/CIGS interface[10–12] mainly containing Na, Cu, O, and Cl impurities. Therefore, a detailed knowledge of the role of point defects and impurities in this material is of key importance. In this contribution, we present a complete assessment of intrinsic and extrinsic point defects in In_2S_3.[13–15]

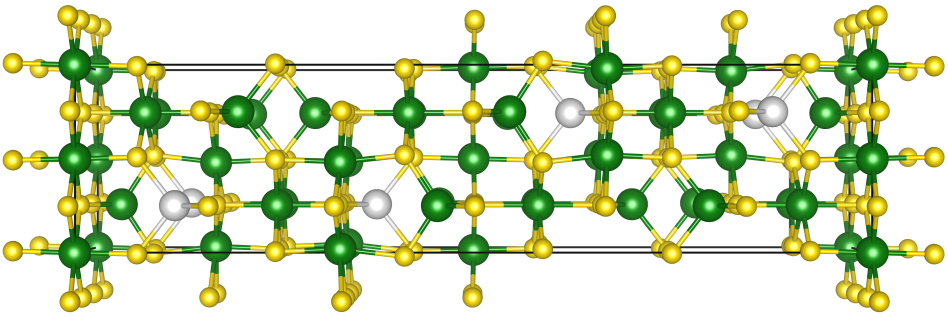

Figure 1. Crystal structure showing the unit cell of β-In_2S_3. Green and yellow spheres represent In and S atoms respectively. The tetrahedral structural vacancies are shown as white spheres (taken from Ref. 13).

2 Methodology

All calculations were carried out within the framework of density functional theory (DFT) using a hybrid functional approach[16] as implemented in the Vienna Ab initio Simulation Package (VASP).[17, 18] For an accurate description of the formation energies, as well as atomic and electronic structures, 25% of non-local Hartree-Fock screened exchange (also known as mixing parameter, α) has been added to 75% of the semi-local exchange energy of PBE functional. The screening range of the electron interaction has been treated by adjusting the Thomas-Fermi screening parameter (w) to 0.13 $Å^{-1}$. The Kohn-Sham equations were solved through employing the projector augmented-wave method,[19, 20] expanding the wave functions up to a cut-off energy of 300 eV. Spin-polarised calculations have been performed for systems with unpaired spins. Defect properties were investigated using a 2×2×1 supercell containing 320 atoms, and the Brillouin-zone sampling was performed using a Γ-centred tetragonal mesh of 2×2×1.

Point defect formation energies have been calculated at theoretical equilibrium volume as

$$E_f[d^q] = \Delta E[d^q] \pm \Sigma_i n_i \mu_i + q[E_{\mathrm{VBM}} + \mu_e] + E_{corr} \quad (1)$$

Since the changes in volume and entropy are tiny in the dilute regime, the effects of formation volume and formation entropy have been skipped in this study. In all calculations the Hellmann-Feynman force convergence was reached only when the largest residual force component on each atom falls below 0.05 eV/Å. $\Delta E[d^q]$ is the energy difference between defect-free and defect-containing structures. n_i corresponds to the number of atoms added or removed from the system. $\mu_i = \mu_i^{ref} + \Delta\mu_i$ is the chemical potential of the constituent i in the reservoir, where μ_i^{ref} denotes the chemical potential of the constituent elements in their stable elemental phases. E_{VBM} is the energy of the valence band maximum (VBM) of the ideal supercell and μ_e is the chemical potential of electrons with respect to E_{VBM}, also known as Fermi level. E_{corr} stands for the artificial electrostatic interactions of point defects with their periodic images and the introduced background charge, which are corrected using FNV scheme provided by Freysoldt, Neugebauer, and Van de Walle.[21, 22]

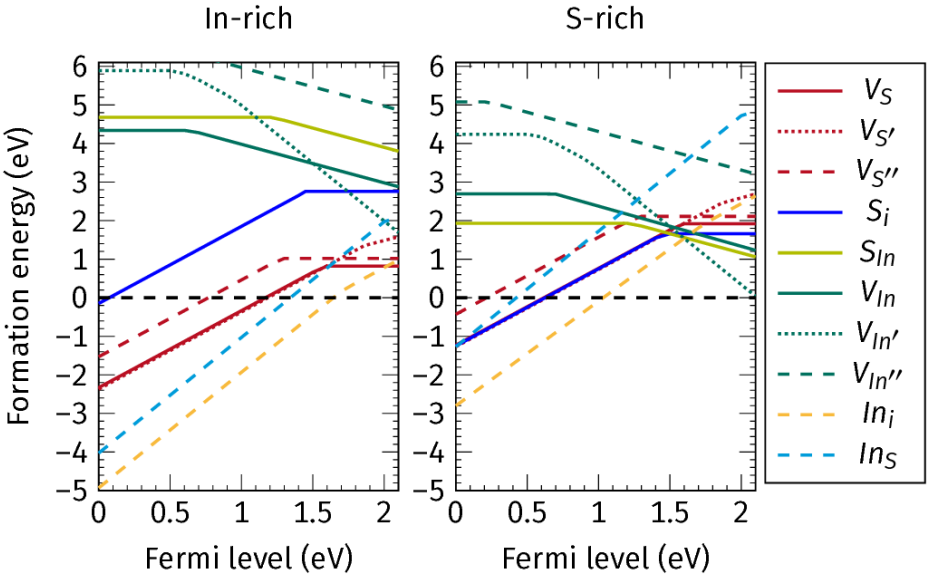

Figure 2. The calculated formation energies of indium and sulphur vacancies as a function of the chemical potential of the electrons, E_f, where E_f=0 eV and E_f=2.1 eV correspond to p-type and n-type conditions, respectively (taken from Ref. 13).

3 The Origin of the n-Type Conductivity of In_2S_3

For obtaining a comprehensive understanding of the role of point defects in indium sulphide, we have calculated formation energies of vacancies (V_S and V_{In}), self-interstitials (S_i and In_i) and anti-sites (S_{In} and In_S) defects as a function of the Fermi level under In-rich and S-rich growth conditions, as shown in Fig. 2. The formation energies shown in Fig. 2 are plotted for the entire range of possible Fermi levels representing various doping conditions. Charge transition levels are positions at points, where the slope of the calculated formation energy changes.

There are three non-equivalent crystallographic environments for indium and sulphur atoms in the β-phase of In_2S_3. The indium substitutional sites in the crystalline matrix of In_2S_3 are tetrahedral $8e$ (denoted In in the following), octahedral $8c$ (denoted In′), and octahedral $16h$ (denoted In″). In a similar fashion, the three different sulphur sites are shown by S (four-fold coordinated to one In, two In′, and one In″), S′ (three-fold coordinated to one In and two In″), and S″ (four-fold coordinated to one In and three In″).

We can see from Fig. 2 that for In-rich samples, there is a strong preference for creation of sulphur vacancies over indium vacancies under both p-type and n-type conditions. However, for S-rich samples, as the Fermi level raises towards the conduction band minimum (CBM), the formation energies and consequently the concentrations of vacant sulphur and vacant indium sites follow a reverse trend. In In-rich samples, the indium interstitial located on the position of a tetrahedral structural vacancy (In_i) has the lowest formation energy at the VBM, lower than all other intrinsic defects. The formation energy of the

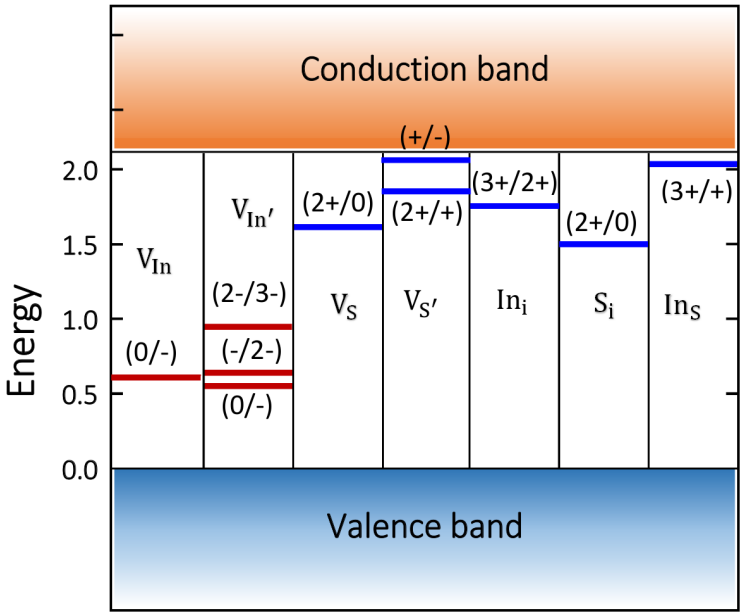

Figure 3. Calculated defect charge transition energies formed in the band gap of β-In_2S_3 using the HSE06[13] functional.

sulphur vacancy (V_S) under the same condition is 0.82 eV. Accordingly, In_i and V_S may play a significant role under thermodynamic equilibrium conditions.

In order to reveal the influence of defects on the electronic structure of the buffer layer, we now discuss the position of charge transition levels as shown in Fig. 3. We see from Fig. 3 that indium vacancies create acceptor levels. However, none of the induced acceptor levels are shallow enough to ionise at room temperature. In S-rich samples, indium atoms need to attain less energy in order to form a vacancy. Consequently, the introduced acceptor levels can be destructive for carrier transport through producing p-conductive acceptor levels. In contrast to indium vacancies, which adopt an acceptor configuration, sulphur vacancies produce donor levels acting as hole killers.

The hybrid functional calculations show that indium in the In_S configuration produces a very shallow (3+/+) donor level at 2.01 eV and a (+/0) level at 0.21 eV above the CBM. Therefore, these intrinsic donor levels can get easily ionised and donate electrons to the conduction band. In_i has also (2+/+) and (+/0) donor levels at 0.03 eV and 0.95 eV above the CBM, which are both resonant within the host bands and can ionise spontaneously, releasing electrons to the system. In consequence, excess indium on anti-sites and tetrahedral vacancies are the main electron-producers, which can effectively dope the material n-type. Besides In_S and In_i, $V_{S'}$ contributes to the n-type conductivity of the system via creating a shallow (+/-) donor-to-acceptor transition level at 0.03 eV below the conduction band. The shallow nature of the (+/-) level allows it to release the two captured electrons at very low temperatures and further boost the free-electron population in the β-In_2S_3.

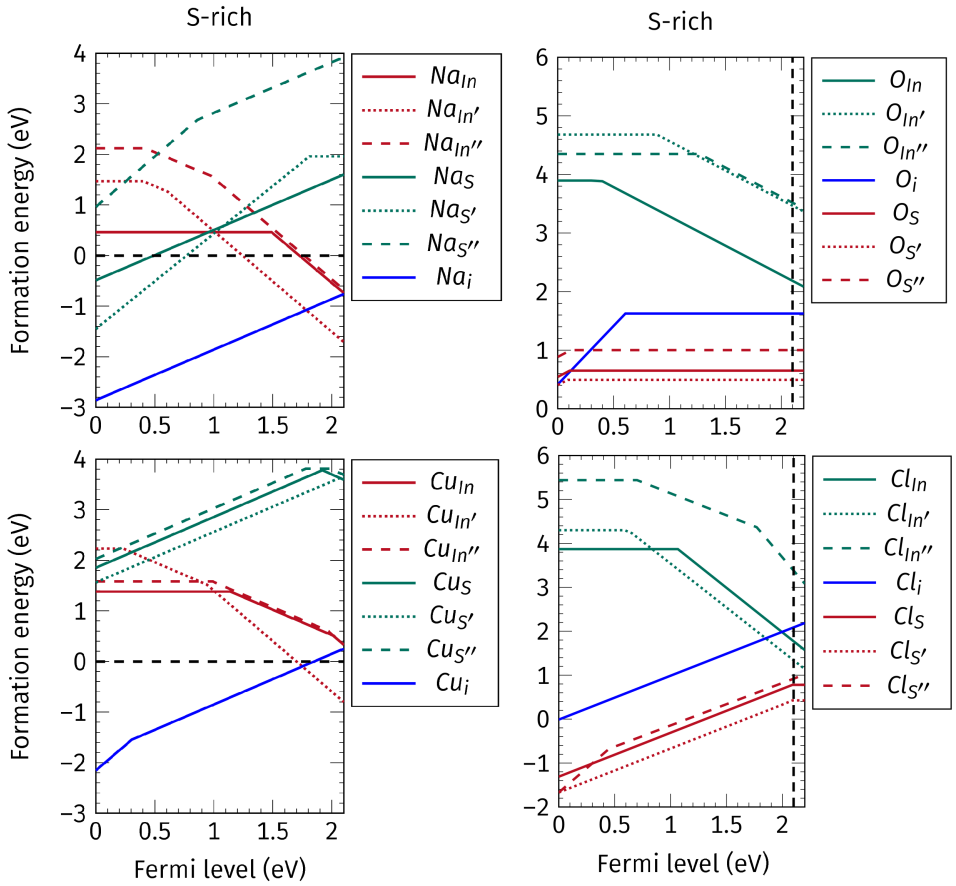

Figure 4. The calculated formation energies of sodium (upper-left), copper (bottom-left), oxygen (upper-right), and chlorine (bottom-right) as a function of the chemical potential of the electrons μ_e, where μ_e=0 eV and μ_e=2.1 eV correspond to p-type and n-type conditions, respectively (taken from Refs. 14, 15).

4 Influence of Impurities on Thermodynamic Stability and Electronic Properties of In_2S_3

When indium sulphide is deposited on CIGS, interdiffusion of Na and Cu from the absorber into the buffer layer leads to the formation of an intermixed absorber-buffer interface involving a high concentration of Na and Cu. Depending on the preparation technique, the presence of O atoms in In_2S_3 may, for instance, stem from side reactions involving decomposition of indium acetylacetonate (used as precursor in the atomic layer deposition (ALD) technique)[23] or high amounts of hydroxide formed during chemical bath deposition (CBD).[23, 24] A significant amount of Cl in In_2S_3 is also detected in the films grown using a Cl-containing precursor (for instance $InCl_3$). In order to put these experimental findings into the context of our theoretical calculations, we have studied the formation enthalpy of Na, Cu, O, and Cl in substitutional and interstitial sites of In_2S_3.[14, 15] Fig. 4 shows the

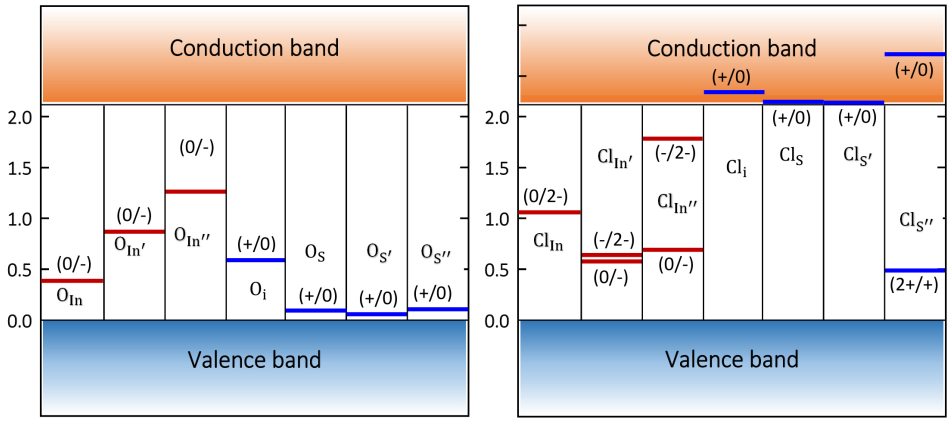

Figure 5. The calculated thermodynamic charge transition levels of O and Cl in different lattice sites of the In_2S_3 (taken from Ref. 15).

calculated formation energies of extrinsic defects in various lattice sites of In_2S_3.

As it can be seen in Fig. 4, the formation enthalpy of Na in the tetrahedral vacancy is negative under both p-type and n-type conditions; this finding unfolds the instability of the system when it comes into contact with a Na reservoir. By Na diffusion into In_2S_3, the system releases energy, and consequently there is a major driving force that triggers the occurrence of side reactions and formation of a Na-containing, interfacial secondary phase on the buffer-side. As a result, the CIGS-In_2S_3 interface is thermodynamically unstable if a Na supply exists in the structure of the multilayer system (*e. g.* Na-containing substrate).

For Cu a slightly different scenario emerges. As long as the Fermi level lies close to the CBM, In_2S_3 can take up a considerable amount of Cu without forming any secondary phases, such as $CuIn_5S_8$; note that the formation energy of Cu_i is positive close to the CBM. However, then the system becomes unstable with respect to Cu_{In} antisite formation, and there is only a small stability window for In-rich conditions, which are experimentally not met. Thus, in the presence of a Cu reservoir, *i. e.* the absorber layer, there is a strong driving force to chemical modifications of the buffer layer. Thus, we can conclude from our data that a thermodynamically stable CIGS-In_2S_3 interface cannot be formed.

Oxygen atoms prefer to occupy S sites rather than In sites. Under n-type conditions, the formation energies of O_S, $O_{S'}$ and $O_{S''}$ are 0.76 eV, 0.49 eV, and 1.0 eV respectively. The very low formation energies of O on different S sites indicates that O substituting anionic sites can occur in In_2S_3 as intrinsic defects. On the Cl side, we see from Fig. 4 that the formation of Cl on sulphur sites is energetically favourable, allowing for a high solubility of Cl in the anionic sub-lattices of In_2S_3. For n-type In_2S_3, the isolated Cl ions on different S sites have formation energies below 1.0 eV, implying that significant concentrations of Cl on S lattice sites can be obtained. $Cl_{S''}$ forms an extremely deep (2+/+) donor state at 1.53 eV below the CBM, and a shallow resonant (+/0) level at 0.65 eV above the CBM, which can readily release electrons to the system.

Fig. 5 shows the calculated charge transition levels for O- and Cl-related point defects. It is seen that O on all S sites induces an extremely deep (+/0) donor level close to the VBM.

The (+/0) level for all three substitutional O on S sites have ionisation energies of around 2.0 eV. In order to effectively dope electrons to the system, donor levels are expected to form near the CBM. However, these deep lying (+/0) levels can neither deliver electrons to the CB nor trap the free holes. In principle, impurity levels close to the valence band can capture free holes. However, since In_2S_3 is an n-type material, the Fermi level lies in the upper part of the band gap. Therefore, the (+/0) levels cannot remove a hole from the valence band. Cl_S and $Cl_{S'}$ induce slight resonances in the conduction band continua, giving rise to a hydrogenic-like (+/0) transition level. The fact that Cl on S sites acts as a shallow donor, suggests that Cl is a suitable n-type dopant in In_2S_3. Therefore, while O on S sites is electrically inactive, Cl on S sites plays a beneficial role in enhancing the concentration of free electrons. This finding allows us to conclude that under low sulphur pressure, intentional doping of In_2S_3 with Cl is an effective way to achieve high levels of n-type conductivity.

5 Concluding Remarks

The formation enthalpy, equilibrium defect transition levels and doping behaviour of a series of native defects and impurities have been studied for bulk β-In_2S_3. Our calculations were done for $2\times2\times1$ supercells containing 320 atoms by means of hybrid functional calculations. Based on our calculations, we identify In_S, In_i, and $V_{S'}$ as dominant sources of n-type conductivity in β-In_2S_3. To understand the stability of the In_2S_3-CIGS interface, we studied the inclusion of extrinsic defects in the In_2S_3 buffer layer. We found that there is a massive driving force for the occurrence of side reactions leading to the formation of Na-containing and Cu-containing interfacial secondary phases. Accordingly, we conclude that the absorber-buffer interface is thermodynamically unstable against the diffusion of Na and Cu into In_2S_3. With regard to the positive formation energies of O- and Cl-related impurities in the crystalline matrix of In_2S_3, we conclude that these anionic impurities do not form secondary phases in the buffer side of the pn-junction. Therefore, the absorber-buffer interface is stable against O and Cl. We found that incorporation of O and Cl on the S sites are energetically favourable. However, while O on S sites creates nonconducting (+/0) impurity levels, Cl on S sites induces hydrogenic-like conductive states, which can actively assist in raising the number of free electrons in the Cl-doped samples.

Acknowledgements

This work has been financially supported by German Federal Ministry for Economic Affairs and Energy (BMWi) through EFFCIS project under contract No. 0324076D. The computing time was provided by Jülich Supercomputing Centre (Project HDA30) and Lichtenberg HPC computer resources at TU Darmstadt.

References

1. W. Rehwald and G. Harbeke, *On the conduction mechanism in single crystal β-indium sulfide In_2S_3*, Journal of Physics and Chemistry of Solids **26(8)**, 1309–1324, 1965.

2. P. Pistor, J. M. Merino Alvarez, M. Leon, M. Di Michiel, S. Schorr, R. Klenk, and S. Lehmann, *Structure reinvestigation of α-, β- and γ-In_2S_3*, Acta Crystallogr. Sect. B: Struct. Sci., Cryst. Eng. Mater. **72**, 410–415, 2016.
3. N. Naghavi, S. Spiering, M. Powalla, B. Cavana, and D. Lincot, *High-efficiency copper indium gallium diselenide (CIGS) solar cells with indium sulfide buffer layers deposited by atomic layer chemical vapor deposition (ALCVD)*, Progress in Photovoltaics: Research and Applications **11(7)**, 437–443, 2003.
4. M. A. Green, K. Emery, Y. Hishikawa, W. Warta, and E. D. Dunlop, *Solar cell efficiency tables (version 48)*, Progress in Photovoltaics: Research and Applications **24(7)**, 905–913, 2016.
5. W. Witte, S. Spiering, and D. Hariskos, *Substitution of the CdS buffer layer in CIGS thin-film solar cells*, Duenne Schichten **26(1)**, 23–27, 2014.
6. N. Naghavi, D. Abou-Ras, N. Allsop, N. Barreau, S. Bücheler, A. Ennaoui, C.-H. Fischer, C. Guillen, D. Hariskos, J. Herrero, R. Klenk, K. Kushiya, D. Lincot, R. Menner, T. Nakada, C. Platzer-Björkman, S. Spiering, A.N. Tiwari, and T. Törndahl, *Buffer layers and transparent conducting oxides for chalcopyrite Cu(In,Ga)(S,Se)$_2$ based thin film photovoltaics: present status and current developments*, Progress in Photovoltaics: Research and Applications **18(6)**, 411–433, 2010.
7. R. Nomura, K. Konishi, and H. Matsuda, *Single-source organometallic chemical vapour deposition process for sulphide thin films: Introduction of a new organometallic precursor BunIn(SPri)2 and preparation of In_2S_3 thin films*, Thin Solid Films **198(1)**, 339–345, 1991.
8. J. F. Trigo, B. Asenjo, J. Herrero, and M. T. Gutierrez, *Optical characterization of In_2S_3 solar cell buffer layers grown by chemical bath and physical vapor deposition*, Solar Energy Materials and Solar Cells **92(9)**, 1145–1148, 2008.
9. J. Sterner, J. Malmström, and L. Stolt, *Study on ald In_2S_3/Cu(In,Ga)Se_2 interface formation*, Progress in Photovoltaics: Research and Applications **13(3)**, 179–193, 2005.
10. P. Pistor, R. Caballero, D. Hariskos, V. Izquierdo-Roca, R. Waechter, S. Schorr, and R. Klenk, *Quality and stability of compound indium sulphide as source material for buffer layers in Cu(In,Ga)Se_2 solar cells*, Solar Energy Materials and Solar Cells **93(1)**, 148–152, 2009.
11. M. Bär, N. Allsop, I. Lauermann, and Ch.-H. Fischer, *Deposition of In_2S_3 on Cu(In,Ga)Se_2 thin film solar cell absorbers by spray ion layer gas reaction: Evidence of strong interfacial diffusion*, Applied Physics Letters **90(13)**, 132118, 2007.
12. M. Bär, N. Barreau, F. Couzinie-Devy, L. Weinhardt, R. G. Wilks, J. Kessler, and C. Heske, *Impact of annealing-induced intermixing on the electronic level alignment at the In_2S_3/Cu(In,Ga)Se_2 thin-film solar cell interface*, ACS Applied Materials & Interfaces **8(3)**, 2120–2124, 2016.
13. E. Ghorbani and K. Albe, *Intrinsic point defects in β-In_2S_3 studied by means of hybrid density-functional theory*, Journal of Applied Physics **123(10)**, 103103, 2018.
14. E. Ghorbani and K. Albe, *Influence of Cu and Na incorporation on the thermodynamic stability and electronic properties of β-In_2S_3*, J. Mater. Chem. C **6**, 7226–7231, 2018.
15. E. Ghorbani and K. Albe, *Role of oxygen and chlorine impurities in In_2S_3: A first-principles study*, Phys. Rev. B **98**, 205201, 2018.
16. J. Heyd, G. E. Scuseria, and M. Ernzerhof, *Hybrid functionals based on a screened Coulomb potential*, J. Chem. Phys. **118(18)**, 8207, 2003.

17. G. Kresse and J. Furthmueller, *Efficient iterative schemes for ab initio total-energy calculations using a plane-wave basis set*, Phys. Rev. B **54**, 11169, 1996.
18. G. Kresse and J. Furthmueller, *Efficiency of ab initio total energy calculations for metals and semiconductors using a plane-wave basis set*, Comput. Mater. Sci. **6(1)**, 15, 1996.
19. G. Kresse and D. Joubert, *From ultrasoft pseudopotentials to the projector augmented-wave method*, Phys. Rev. B **59**, 1758, 1999.
20. P. E. Bloechl, *Projector augmented-wave method*, Phys. Rev. B **50**, 17953, 1994.
21. C. Freysoldt, J. Neugebauer, and C. G. Van de Walle, *Fully ab initio finite-size corrections for charged-defect supercell calculations*, Phys. Rev. Lett. **102**, 016402, 2009.
22. C. Freysoldt, J. Neugebauer, and C. G. Van de Walle, *Electrostatic interactions between charged defects in supercells*, physica status solidi (b) **248(5)**, 1067–1076, 2011.
23. N. Naghavi, R. Henriquez, V. Laptev, and D. Lincot, *Growth studies and characterisation of In_2S_3 thin films deposited by atomic layer deposition (ALD)*, Applied Surface Science **222(1–4)**, 65–73, 2004.
24. D. Hariskos, M. Ruckh, U. Ruehle, T. Walter, H. W. Schock, J. Hedstroem, and L. Stolt, *A novel cadmium free buffer layer for $Cu(In,Ga)Se_2$ based solar cells*, Solar Energy Materials and Solar Cells **41**, 345–353, 1996.